H13-46

IMPACT OF BUILDING SEPARATION ON NATURAL VENTILATION BEHAVIOUR AND PERFORMANCE FOR LOW-RISE STRUCTURES

James O.P. Cheung[1], Chun-Ho Liu[1] and Michael C.H. Yam[2]

[1]Department of Mechanical Engineering, The University of Hong Kong
[2]Department of Building and Real Estate, The Hong Kong Polytechnic University

Abstract: Natural ventilation, a readily available natural resource, should be better utilized for integrating the concept of sustainability in our built environment. Obviously, the clearance among buildings is a crucial factor affecting the natural ventilation performance. This paper attempts to reveal the ventilation behaviour in urban geometry of different building spacing. Large-eddy simulations (LES) were performed with the one-equation subgrid-scale (SGS) model for the unresolved turbulent kinetic energy. Three evenly separated two-dimensional (2D) hypothetical buildings were aligned in the streamwise direction that made up the computational domain. Cross-ventilation was enabled by opening up the lower halves of the windward and leeward facades. The Reynolds number was prescribed at around 50,000 to ensure fully developed turbulent flow. The sensitivity of the ventilation rate and the flow pattern in and around the buildings to building separation was examined. Fresh air entrainment from the shear layer aloft was significantly suppressed when the building separation was small. Reversed flow and recirculations were dominated near the ground and within the building envelope. Changes in the flow pattern, such as the positions, the sizes and the intensities of the recirculations, were observed with increasing separation. The contribution of turbulence to the total ventilation rate differed by various extents. When the separation approached 1.5 times the building height, the mean ventilation flux across the building envelope dropped to almost zero while the turbulent flux dominated the ventilation.

Key words: *Building interference, Computational fluid dynamics (CFD), Cross ventilation, Large-eddy simulation, Natural ventilation, Urban geometry*

INTRODUCTION

Unlike mechanical ventilation, natural ventilation offers a number of advantages such as lower power costs and greater health conditions, etc. (Martin and Fitzsimmons 2000, Emmerich *et al.* 2001). The natural ventilation behaviour in the built regions is hard to determine because of the substantial flow modification by buildings. Within a street canyon, the voids are susceptible in trapping ground-level pollutants and suppressing air exchange above the canopy layer. Oke (1988) identified the changes in airflow patterns in the 2D voids with respect to the building-height-to-separation (aspect) ratio (H/W), which are grouped into three categories. Similarly, Chang and Meroney (2003) studied the airflow and pollutant concentrations in street canyons of different aspect ratios using both wind tunnel and computational fluid dynamics (CFD) results. Liu *et al.* (2005) evaluated the air exchange rate using LES. In line with other studies, it was found that the air exchange was more active at smaller aspect ratios. A vast amount of studies emphasizing the pollutant dispersion behaviours in the three characteristic flow regimes have been reported elsewhere (Crowther and Hassan 2002, Yang *et al.* 2007, Cai *et al.* 2008).

The aforementioned papers consistently found that the outdoor environment responds differently to various building separations. The cross-ventilation through an indoor space was therefore expected to change accordingly. However, the research effort dedicated to that area is surprisingly small. Only a handful of papers, such as Syrios and Hunt (2008) and Cheung and Liu (2009), have been conducted to study the effects of separation on buoyancy- and wind-driven cross ventilation. These papers hinted a need to explore how building natural ventilation is affected by the outdoor environment.

Since the 1980s, comparisons of CFD results with measurements have proved the superior accuracy of LES (Sakamoto and Matsuo 1980, Kato *et al.* 2002). Cheng *et al.* (2003) demonstrated the outstanding performance of LES in calculating the flow features, the mean velocities, and the Reynolds stresses. LES also capture well the transient characteristics of the flow variables that are particularly useful if the turbulent parts of the studied parameters are important. As such, LES was employed in this paper to address the ventilation performance of low-rise buildings within street canyons of various aspect ratios.

MATHEMATICAL MODEL

LES with the one-equation SGS TKE model for k_{sgs} (Schumann 1975) was applied. The filtered continuity and Navier-Stokes equations were solved. An additional equation was included to calculate the conservation of the SGS TKE.

$$\frac{\partial k_{sgs}}{\partial t} + \frac{\partial}{\partial x_j}(\overline{u_i} k_{sgs}) = \frac{\partial}{\partial x_j}(\nu_{eff} \frac{\partial k_{sgs}}{\partial x_j}) + \nu_{sgs} \overline{S}^2 (k_{sgs})^{3/2} / \Delta \quad (1)$$

The variables with overlines are the filtered quantities. ν_{eff} and ν_{sgs} are, respectively, the effective and subgrid-scale viscosity. Δ is the filter width and $\bar{S} = 0.5(\partial \overline{u_i}/\partial x_j + \partial \overline{u_j}/\partial x_i)$ is the resolved strain rate tensor. The governing equations were solved by the finite volume method (FVM). The second-order accurate backward differencing scheme was employed for the time derivative. The second-order accurate central differencing scheme, which is more accurate than the lower-order upwind scheme (Zhang and Chen 2000, Denev *et al.* 2004) for LES applications, in conjunction with Gaussian discretization was used for the spatial derivatives. All simulations were performed using the open-source CFD code OpenFOAM (2010).

LES MODEL VALIDATION

Our preliminary results using a LES with the standard Smagorinsky SGS model suffered from deviations in the predicted sizes and locations of characteristic flow features compared with the wind tunnel measurements. Some previous studies noticed the deficiency of the standard Smagorinsky SGS model, and commented that the uniform Smagorinsky constant

throughout the whole domain is prone to the aforementioned error (Davidson and Nielson 1996, Jiang and Chen 2001). Therefore, in this paper, the one-equation SGS model for k_{sgs} was adopted. A quantitative comparison on the airflow inside and around a cross-ventilated cubic building (Jiang *et al.* 2003) is reported below. The CFD domain sized $11H \times 6H \times 4H$ (length × width × height). Random perturbations of 10% were introduced into the mean velocity profile as artificial turbulence. The streamwise and vertical velocities along five profiles on the selected vertical $(x-z)$ centre-plane were compared (Figure1).

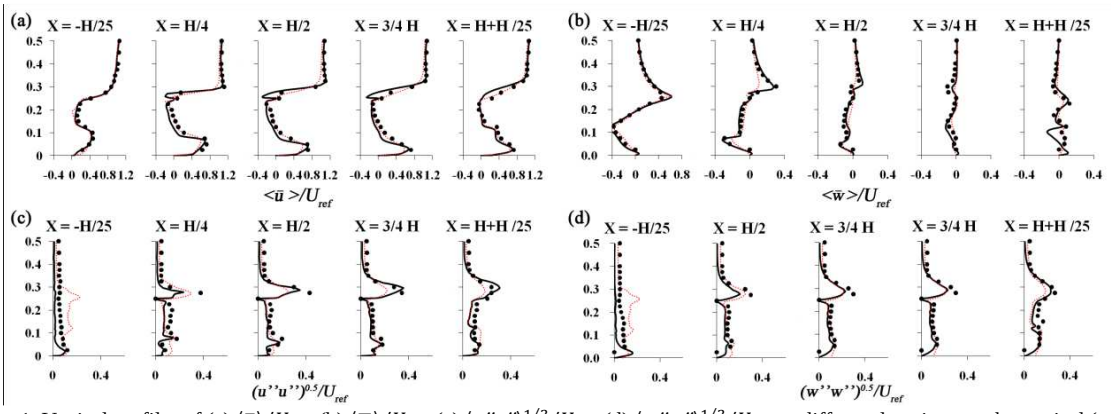

Figure 1. Vertical profiles of (a) $\langle\bar{u}\rangle/U_{ref}$ (b) $\langle\bar{w}\rangle/U_{ref}$ (c) $\langle u''u''\rangle^{1/2}/U_{ref}$ (d) $\langle w''w''\rangle^{1/2}/U_{ref}$ at different locations on the vertical $(x-z)$ centreplane (Solid lines: LES; red dotted lines: $k-\varepsilon$ turbulence model; black dots: wind tunnel results from Jiang *et al.* 2003)

Figures 1a and 1b compare the mean streamwise ($\langle\bar{u}\rangle/U_{ref}$) and vertical ($\langle\bar{w}\rangle/U_{ref}$) velocities obtained from the current LES, our previous $k-\varepsilon$ turbulence model, and the measurement (Jiang *et al.* 2003). The basic characteristics, such as the separation and the flow through the buildings, were successfully calculated. Except near the roof where a slight under-prediction was observed, the performance of LES was ascertained. The difference could be caused by the sensitivity of LES to the spatial resolution. The LES also outperformed the $k-\varepsilon$ model in predicting $\bar{w}$, especially inside and above the building model. The fluctuating streamwise ($\langle u''u''\rangle^{1/2}/U_{ref}$) and vertical ($\langle w''w''\rangle^{1/2}/U_{ref}$) velocity components both demonstrated good agreements with the experimental data (Figures 1c and 1d). The under-prediction upstream of the building was caused by the dissimilarity in turbulence activation at the inflow. Otherwise, the strength and distribution of turbulence were compared reasonably well in the experimental observations. A high level of turbulences was observed within and behind the roof recirculation and at the door-level. The profiles of fluctuating velocity from the $k-\varepsilon$ turbulence model were calculated by assuming anisotropic turbulence. The characteristic of over-estimated turbulence level around the windward façade was diminished in the LES. The pressure distribution on the façades proves that the LES results were comparable to the wind tunnel measurements (Figure 2).

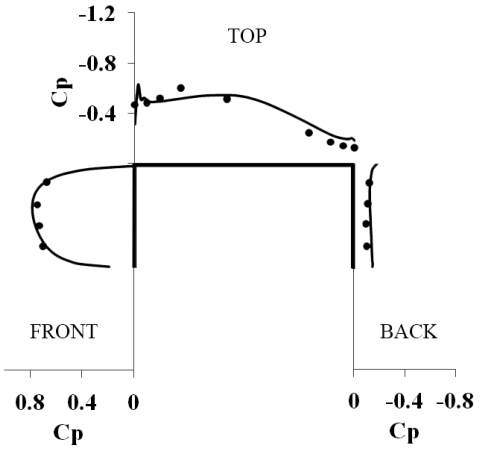

Figure 2. Mean pressure coefficient C_p on the façades (Solid lines: LES; black dots: wind tunnel results from Jiang *et al.* 2003)

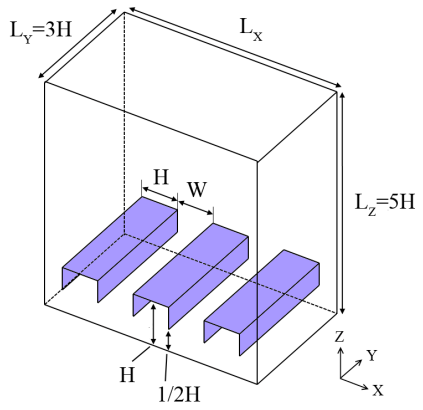

Figure 3. The computational domain

COMPUTATIONAL DOMAIN

In our natural ventilation study, the computational domain was composed of three 2D hypothetical square buildings of size $H \times H$ (width × height) mounted on the floor and separated evenly at distance W (Figure 3). The lower halves of the windward and leeward walls were opened facilitating cross-ventilation across the buildings. A total of four aspect ratios, $H/W = 1, 0.67, 0.5$ and 0.25, were examined. The domain geometry was homogenous in the spanwise direction, spanning a length of $3H$. The height of the computational domain measured $5H$. The domain was discretized by structural meshes into four to six million cells, depending on W. The finest meshes of length scale $0.008H$ were located near the openings.

The streamwise and spanwise directions were assumed to be periodic for momentum. Neumann conditions were used at the top boundary. The ground and all the walls were prescribed with no-slip boundary conditions. A pressure gradient term $\langle P \rangle$ was applied to the filtered momentum equation, forcing the movement of air in the streamwise direction in the shear layer above the roof-level (from H to $5H$). The Reynolds number at the roof-level was kept at around 50,000. The calculated flow variables were normalized by the corresponding reference values taken at $Z = 1.2H$. The simulations are currently still in progress. In the following section, only the available preliminary results are reported.

DISCUSSION OF RESULTS

Starting from the largest aspect ratio, $H/W = 1$, the ensemble average streamwise ($\langle \overline{u} \rangle / U_{ref}$) and spanwise ($\langle \overline{w} \rangle / U_{ref}$) velocities together with streamline analysis are shown in Figures 4 and 5 respectively. At the roof level, the flow in the shear layer gave rise to a roof-level streamwise velocity of around $0.35U_{ref}$ that impinged on the windward façade then directed downward. The air tended to flow towards the leeward side of the upwind building, forming a large clockwise recirculation occupying most space of the street canyon. This recirculation induced a negative $\langle \overline{u} \rangle$ near the ground level. From $Z = 0$ to $0.6H$, $\langle \overline{u} \rangle$ ranged from 0 to $-0.1U_{ref}$. The negative streamwise flow is also dominated inside the building from the ground to $Z = 0.7H$. The buildings were thus ventilated by the reversed airflow entering from the leeward openings. It is also worth mentioning that the air velocity was rather low indoors (within $0.15U_{ref}$). Figures 6 and 7 depict the velocity fluctuations. Similar to the mean flow properties, $\langle u''u'' \rangle^{1/2}/U_{ref}$ is elevated in the shear layer close to the roof level, whereas the maxima of $\langle w''w'' \rangle^{1/2}/U_{ref}$ occurred near the windward façade. The fluctuations were stronger at the leeward opening that were promoted to about $0.1U_{ref}$ that was comparable to the respective resolved mean values.

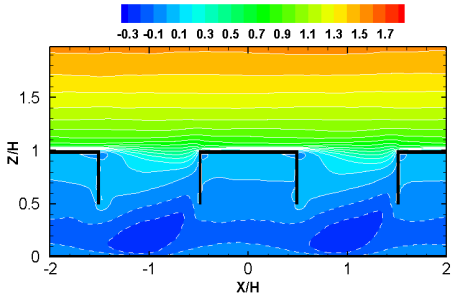

Figure 4. Mean streamwise velocity ($\langle \overline{u} \rangle / U_{ref}$) at $H/W = 1$

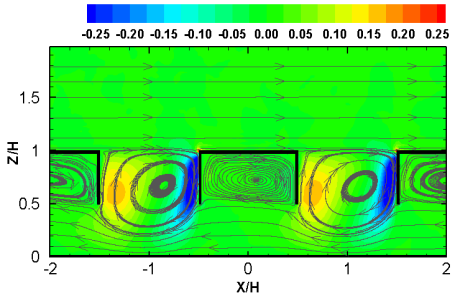

Figure 5. Mean vertical velocity ($\langle \overline{w} \rangle / U_{ref}$) at $H/W = 1$

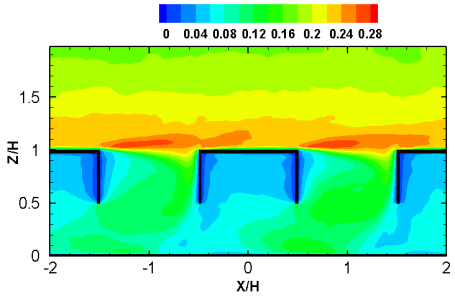

Figure 6. Streamwise fluctuations ($\langle u''u'' \rangle^{1/2}/U_{ref}$) at $H/W = 1$

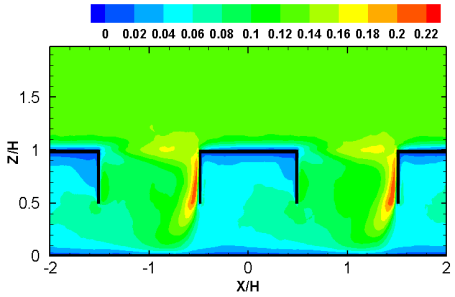

Figure 7. Vertical fluctuations ($\langle w''w'' \rangle^{1/2}/U_{ref}$) at $H/W = 1$

As the separation was enlarged to $H/W = 0.5$, the ventilation mechanism changed significantly with air ventilating the building in the positive streamwise direction (Figures 8 and 9). The large recirculation in the canyon still persisted, covering a streamwise distance of about $1.25H$. Next to the windward façade, the downward flow was strengthened to around $-0.55U_{ref}$, entraining down to the ground level. Part of the flow recirculated forming the aforementioned recirculation, while the remaining penetrated the windward opening and exited through the leeward one, characterising a typical cross-ventilation configuration. This cross-ventilation led to the formation of an anti-clockwise recirculation inside the building. The indoor velocities were generally over $0.1U_{ref}$, going as high as $0.5U_{ref}$ near the ground, hinting a more complete air mixing than the previous cases of $H/W = 1$. After exiting from the leeward opening, the air was carried upward to the roof level arriving the windward end of the large clockwise recirculation. Similar to the case of $H/W = 1$, stronger fluctuations occurred at the roof-level and around the windward façade (Figure 10). The amplitude was also larger for a wider separation; for example, $\langle w''w'' \rangle^{1/2}$ reached $0.2U_{ref}$ at the windward opening (Figure 11), compared with only $0.05U_{ref}$ at $H/W = 1$. This suggested a more active exchange of air and a more effective pollutant removal as well.

Figures 12 to 15 illustrate the mean and turbulent parts of the airflow at the two openings. It is clearly observed that both the magnitudes of mean flow and fluctuations were smaller at $H/W = 1$ that was in line with our general perception on the effect of high aspect ratio. Furthermore, when the aspect ratio was large, $\langle u''u'' \rangle^{1/2}$ and $\langle w''w'' \rangle^{1/2}$ were generally higher than their $\langle \overline{u} \rangle$ and $\langle \overline{w} \rangle$ counterparts. For instance, at the leeward opening, the averaged $\langle u''u'' \rangle^{1/2}/U_{ref}$ and $\langle w''w'' \rangle^{1/2}/U_{ref}$ were up to 115% and 153% respectively. The fluctuating part was less dominant at $H/W = 0.5$ with reduced $\langle u''u'' \rangle^{1/2}$ (= 101%) and $\langle w''w'' \rangle^{1/2}$ (=69%) accordingly. It is believed that the contribution from mean flow overrides that from turbulence

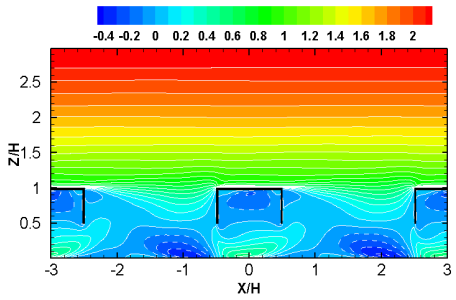

Figure 8. Streamwise velocity ($\langle\bar{u}\rangle/U_{ref}$) at $H/W = 0.5$

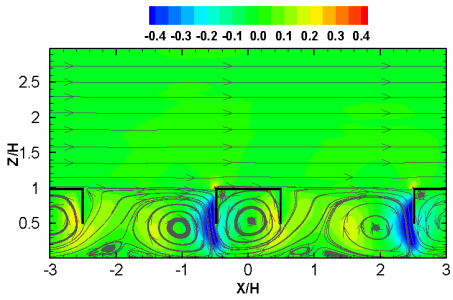

Figure 9. Vertical velocity ($\langle\bar{w}\rangle/U_{ref}$) at $H/W = 0.5$

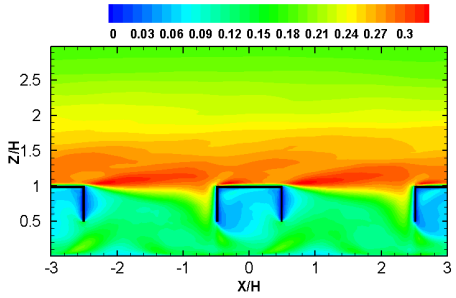

Figure 10. Streamwise fluctuations ($\langle u''u''\rangle^{1/2}/U_{ref}$) at $H/W = 0.5$

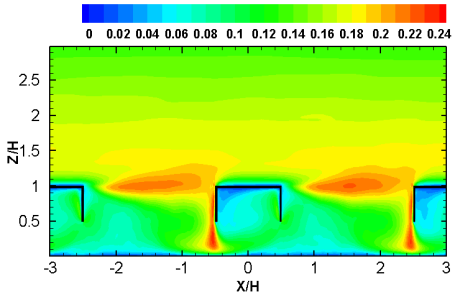

Figure 11. Vertical fluctuations ($\langle w''w''\rangle^{1/2}/U_{ref}$) at $H/W = 0.5$

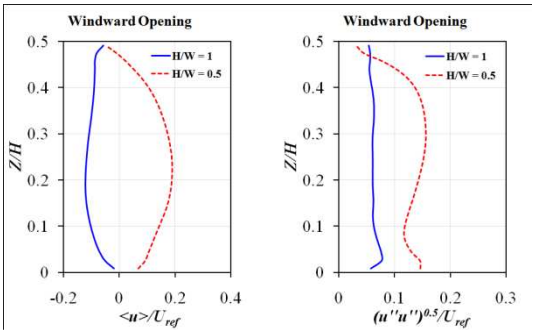

Figure 12. $\langle\bar{u}\rangle/U_{ref}$ and $\langle u''u''\rangle^{1/2}/U_{ref}$ at the windward opening

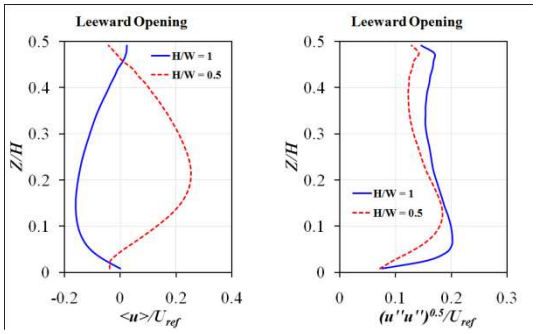

Figure 13. $\langle\bar{u}\rangle/U_{ref}$ and $\langle u''u''\rangle^{1/2}/U_{ref}$ at the leeward opening

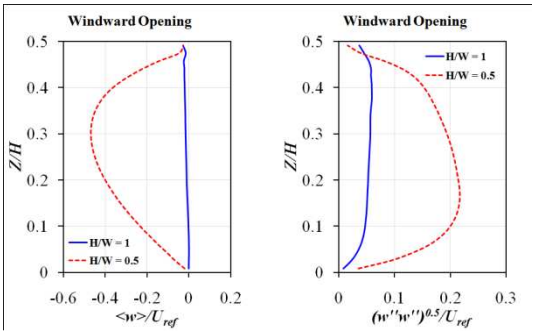

Figure 14. $\langle\bar{w}\rangle/U_{ref}$ and $\langle w''w''\rangle^{1/2}/U_{ref}$ at the windward opening

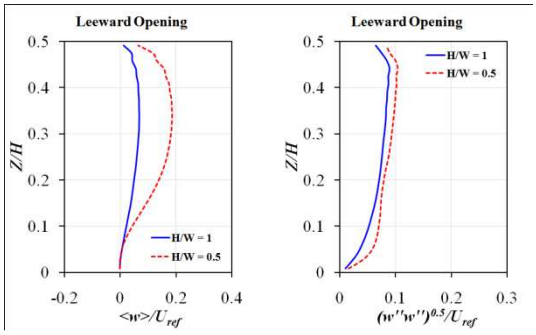

Figure 15. $\langle\bar{w}\rangle/U_{ref}$ and $\langle w''w''\rangle^{1/2}/U_{ref}$ at the leeward opening

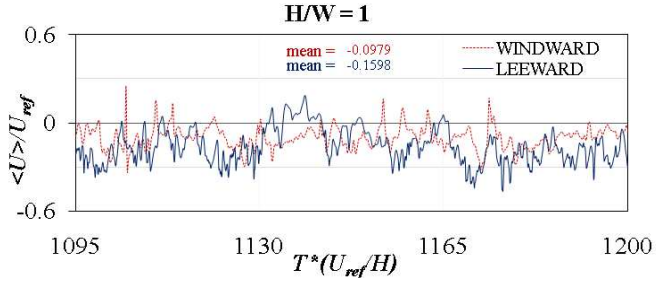

Figure 16. Time series of streamwise velocity ($\langle\bar{u}\rangle/U_{ref}$) at the centre of the openings at $H/W = 1$

at decreasing aspect ratio. Figure 16 demonstrates the significance of turbulence at $\boldsymbol{H/W = 1}$ by showing a time series of instantaneous streamwise velocity at the centre of the openings.

SUMMARY

The more reliable LES with the one-equation model for SGS kinetic energy was used to study the cross-ventilation in buildings placed at four different aspect ratios ($H/W = 1, 0.67, 0.5$ and 0.25). Two of them ($H/W = 1$ and 0.5) were discussed in this paper. The cross-ventilation rates and mechanisms were compared.

1. Different flow mechanisms were observed for the two aspect ratios discussed. The mean flow through the buildings was in reversed direction with respect to the prevalent wind at $H/W = 1$. At $H/W = 0.5$, prevalent wind from the shear layer could reach the windward opening and passed through the buildings, the mean streamwise velocity thus reverted to positive, i.e. typical cross-ventilation configuration.
2. The averaged flow speed inside the building also varied, from below to above $0.1U_{ref}$ when H/W is reduced from 1 to 0.5. This finding agreed with the general concept that the ventilation rate is higher for canyons at wider separation. Fresh air entrainment from the shear layer was more vigorous at lower aspect ratio, as suggested by the higher value of $\langle w''w'' \rangle^{1/2}$ at the roof level at $H/W = 0.5$.
3. On average, the turbulence intensity at the openings was greater at $H/W = 1$. The contribution of turbulence in ventilation was significant at a smaller separation, suggesting its importance in natural ventilation estimate.

The simulations for the remaining aspect ratios, $H/W = 0.67$ and 0.25, are undertaken. Preliminary observations include the near-zero mean flow across the windward opening at $H/W = 0.67$. Ventilation is dominated by turbulence fluctuations. The results will be discussed in the upcoming papers. This paper enriched an in-depth understanding on how natural ventilation works in buildings of different densities. Further studies are encouraged to better utilize our natural wind resources.

REFERENCES

Cai, X.-M. Barlow, J.F. and Belcher, S.E., 2008: Dispersion and transfer of passive scalars in and above street canyons—Large-eddy simulations, *Atmos. Environ.*, **42**, 5885-5895.

Chang, C.-H. and Meroney, R.N., 2003: The effect of surroundings with different separation distances on surface pressures on low-rise buildings, *J. Wind Eng. Ind. Aerodyn.*, **91**, 1039–1050.

Cheng, Y., Lien, F.S., Yee, E. and Sinclair, R., 2003: A comparison of large Eddy simulations with a standard k–ε Reynolds-averaged Navier–Stokes model for the prediction of a fully developed turbulent flow over a matrix of cubes, *J. Wind Eng. Ind. Aerodyn.*, **91**, 1301-1328.

Cheung, J.O.P. and Liu, C.-H., 2009: Effects of Building Interference on Natural Ventilation for High-Rise Residential Buildings, *Proceedings of the 6th International Symposium on Heating, Ventilating and Air Conditioning*, **2**, 1276-1283.

Crowther, J.M. and Hassan, A.G.A.A., 2002: Three-Dimensional Numerical Simulation of Air Pollutant Dispersion in Street Canyons, *Water Air Soil Pollut. Focus*, **2**, 279-295.

Davidson, L. and Nielson, P.V., 1996: Large Eddy Simulations of the Flow in a Three-Dimensional Ventilated Room, *5th Int. Conf. on Air Distributions in Rooms ROOMVENT '96*, **2**, 161-168.

Denev, J., Frank, T. and Pachler, K., 2004: Large Eddy Simulation of Turbulent Square Channel Flow Using a PC-Cluster Architecture, Lecture notes in computer science, 363-370.

Emmerich, S.J., Dols, W.S. and Axley, J.W., 2001: Natural Ventilation Review and Plan for Design and Analysis Tools, NISTIR 6781, National Institute of Standards and Technology, Technology Administration, U.S. Department of Commerce.

Jiang, Y. and Chen, Q., 2001: Study of natural ventilation in buildings by large eddy simulation, *J. Wind Eng. Ind. Aerodyn.*, **89**, 1155-1178.

Jiang, Y., Alexander, D., Jenkins, H., Arthur, R. and Chen, Q., 2003: Natural ventilation in buildings: measurement in a wind tunnel and numerical simulation with large-eddy simulation, *J. Wind Eng. Ind. Aerodyn.*, **91**, 331–353.

Kato, S., Murakami, S., Mochida, A., Akabayashi, S.-I. and Tominaga, Y., 1992: Velocity-pressure field of cross ventilation with open windows analyzed by wind tunnel and numerical simulation, *J. Wind Eng. Ind. Aerodyn.*, **44**, 2575-2586.

Liu, C.-H., Leung, D.Y.C. and Barth, M.C., 2005: On the prediction of air and pollutant exchange rates in street canyons of different aspect ratios using large-eddy simulation, *Atmos. Environ.*, **3**, 1567-1574.

Martin, A. and Fitzsimmons, J., 2000: Making natural ventilation work, BSRIA (GN 7/2000), Bracknell, Berkshire.

Oke, T.R., 1988: Street design and urban canopy layer climate, *Energy Build*, **11**, 103–113.

OpenFOAM, 2001: OpenFOAM® - The Open Source Computational Fluid Dynamics (CFD) Toolbox, http://www.openfoam.com/

Sakamoto, Y. and Matsuo, Y., 1980: Numerical predictions of three-dimensional flow in a ventilated room using turbulence models, *Appl. Math. Modelling*, **4**, 67-72.

Schumann, U., 1975: Subgrid scale model for finite difference simulations of turbulent flows in plane channels and annuli, *J. Comput. Phys.*, **18**, 376-404.

Syrios, K. and Hunt, G.R., 2008: Passive air exchanges between building and urban canyon via openings in a single facade, *Int. J. Heat Fluid Flow*, **29**, 364–373.

Yang, R., Zhang, J., Shen, S., Li, X. and Chen, J., 2007: Numerical Investigation of the Impact of Different Configurations and Aspect Ratios on Dense Gas Dispersion in Urban Street Canyons, *Tsinghua Sci. Technol.*, **12**, 345-351.

Zhang, W. and Chen, Q., 2000: Large eddy simulation of indoor airfow with a filtered dynamic subgrid scale model, *Int. J. Heat Mass Transfer*, **43**, 3219-3231.